

# Integrated rainfall–runoff and flood inundation modeling for flash flood risk assessment under data scarcity in arid regions: Wadi Fatimah basin case study, Saudi Arabia

Amro Elfeki<sup>1</sup>  · Milad Masoud<sup>2</sup> · Burhan Niyazi<sup>1,2</sup>

Received: 18 June 2015 / Accepted: 27 August 2016 / Published online: 1 September 2016  
© Springer Science+Business Media Dordrecht 2016

**Abstract** This paper presents a proposed integrated approach for flood hazardous evaluation in arid and semi-arid areas. Wadi Fatimah in Saudi Arabia is utilized for implementation of such an approach. The approach consists of four stages. In the first stage, a statistical analysis of rainfall data is performed to determine the design storms at specified return periods. In the second stage, geological and geomorphologic analyses are followed to estimate the geomorphic parameters. The third stage concerned with land use and land cover analyses linked with hydrological analysis to estimate the hydrographs. The fourth stage is related to the delineation of the inundation area under two scenarios: the presence and absence of the dam. The statistical analysis proved that some rainfall stations do not follow a Gumbel distribution. The presence of the dam reduces the inundation depth by about 10 %. The reduction in the inundation area due the presence of the dam is about 25 %.

**Keywords** Rainfall–runoff modeling · Inundation modeling · Statistical analysis · Flash flood · Wadi Fatimah · Protection dams · Data scarcity · Reservoir routing · Elevation–capacity curve

---

**Electronic supplementary material** The online version of this article (doi:[10.1007/s11069-016-2559-7](https://doi.org/10.1007/s11069-016-2559-7)) contains supplementary material, which is available to authorized users.

---

✉ Amro Elfeki  
elfeki\_amr@yahoo.co.uk

<sup>1</sup> Department of Hydrology and Water Resources Management, Faculty of Meteorology, Environment and Arid Land Agriculture, King Abdulaziz University, P.O. Box 80208, Jeddah 21589, Saudi Arabia

<sup>2</sup> Water Research Center, King Abdulaziz University, P.O. Box 80208, Jeddah 21589, Saudi Arabia

## 1 Introduction

Arid and semi-arid environments endure massive flash floods that cause fatality and damage to infrastructure and properties. Saudi Arabia is an example of arid and semi-arid regions where runoff and drainage basins record are unavailable for most of the basins. There are no runoff gauges installed to measure flood discharge in most of watersheds (wadis) in Saudi Arabia. The term “flash flood” reflects a prompt response, with water levels in the drainage network reaching a peak within minutes to few hours after starting of the rain storm event with extremely very short time of alarming (Georgakakos 1992; Creutin and Borga 2003; Collier 2007; Younis et al. 2008). According to Subyani (2009), arid areas are subjected to flash flood which results from extreme rainfall and leads to destruction of the infrastructures. Flash flood assessment is an important practice, yet it is a difficult task. The main challenge to assess flash flood in such arid and semi-arid area is the limitation or in some cases the absence of the hydrological information.

Rainfall–runoff modeling has become a must for sustainable water resources development and for flood risk and drought management (or protection). Precipitations and surface runoff are the vital hydrological parameters for evaluating and mapping of flash flood. Therefore, it is very important to find alternative methods to model rainfall and runoff when measured hydrological data are not available in the study area (Sen et al. 2012). One of these alternatives is to develop thematic map of flood inundations based on the topographic and morphometric characteristics of the arid basins. Zenger and Smith (2003) reported that the integration between GIS, paleo-flood information and basin physiographic features to assess flash flood risk has been highly developed and common among researchers in the beginning of the twenty-first century due to the progress of spatial data analyst and geoinformatic tools. Many researches dealing with the flood risk evaluation and mapping based upon geoinformatic techniques are, e.g., Sui and Maggio (1999), Merzi and Aktas (2000), Guzzetti, and Tonelli (2004), Sanyal and Lu (2006), He et al. (2003), Fernandez and Lutz (2010) and El Osta and Masoud (2015).

Physiographic features of the drainage basin in many areas of the world have been studied using conventional geomorphologic approaches (Horton 1932, 1945; Strahler 1964; Rudriaih et al. 2008; Al Saud 2009; Nageswararao et al. 2010; Masoud 2015). Al Yamani (2004) has performed a hydrological study on wadi Fatimah basin to evaluate the hydraulic response of the basin. However, his study did not consider flood inundation mapping. Al-Ahmadi (2005) has performed a hydrological study on rainfall–runoff relations in Saudi Arabia using HEC-HEMS and GIS and remote sensing technology. His study is based on data collected in the 1980s and focused on the southwestern part of Saudi Arabia but not wadi Fatimah. Subyani (2009) has studied the hydrological behavior and flood probability for selected arid basins in Makkah Al-Mukaramah area. His study focused on probability distributions of rainfall in the region; however, the author tested only two probability distributions on the data. In the current study, the authors focused on testing five famous distributions and proposed a systematic method to test them. A recent study by Masoud et al. (2014) has focused on mapping of flash flood hazards in wadi Fatimah in the Kingdom of Saudi Arabia based on the integration of physiographic features and GIS techniques. They were able to show a potential hazard degree map within the watershed and specify locations within the wadi for recharge potential.

The target of this study is to present an integrated method based upon coupling of rainfall–runoff model mutually with flood inundation model for the evaluation of flash flood risks in arid environment under data scarcity. The proposed approach consists of four

stages. In the first stage, statistical analysis of rainfall data in space and time is performed to determine design storms at different return periods. In the second stage, geological and geomorphologic analyses are followed to delineate catchment area and stream network in the basin. The third stage dealt with land use and land cover analyses linked with hydrological analysis to estimate the corresponding hydrographs for each return period. The fourth stage focused on the delineation of the inundation area in the upstream and downstream of the dam under two scenarios: the presence of the dam and the absence of the dam. Although this approach seems conventional, to the best of the authors' knowledge, no such studies have been performed in Saudi Arabia. Since there is no runoff measurement available in the study area which is common in arid regions especially in Saudi Arabia, therefore a synthetic hydrograph method (SCS method) is applied for the hydrological analyses. Figure 1 shows the general framework of the proposed integrated approach.

## 2 Location and geology of the study area

Wadi Fatimah covers a large area in the south and eastern part of Jeddah Governorate and extends from NE to SW with 4869 km<sup>2</sup> area (the catchment as a whole with an outlet at the Red Sea). It is located between longitudes 39°15' and 4°30'E and latitudes 21°16' and 22°15'N. The study area is located within Tihama escarpment of the Arabian shield. It is characterized by annual flash floods. Recently, the study area received catastrophic flash floods that happened in November 2009 and December 2010, 2012 and 2013 that caused much damage.

Geologically, the study area consists of Precambrian (Basement), Tertiary rocks, and the Quaternary of alluvial deposits (Fig. 2). Basement rocks of wadi Fatimah cover 63.6 % of the area consisting of Late-Proterozoic basalts to rhyolites volcanic, volcano-clastic and epiclastics of ancient island-arc types that have been distorted, metamorphosed and injected by intrusive bodies of diverse ages and compositions. The Tertiary rocks are exposed beneath the lava and Quaternary deposits on 13.9 % of wadi Fatimah's area. It is composed of clastic rocks of sandstones, shale, mudstones and some of conglomerates. Quaternary deposits occupy great portion of wadi Fatimah basin about 22.5 %, with a range of 2–20 m thickness. These deposits basically occur in the main channels of wadi Fatimah. The Quaternary deposits are composed mainly of gravels, sands, alluvial deposits and wadi beds. Figure 2 shows the location and geology of wadi Fatimah.

## 3 Geomorphology of Wadi Fatimah

The geomorphologic aspects of wadi Fatimah show a classic wadi features extending from western part of the escarpment ridge of the Arabian shield. It begins from the eastern elevated mountain series of steep slope and decreases downward to the western direction at the coastal plain of Tihama region (Masoud 2015, 2016). The altitude of wadi Fatimah ranges from 10 to 2314 m with a mean elevation of 753 m (amsl), as shown in Fig. 3. Wadi Fatimah and its vicinities exhibit different geomorphologic features that can be described as: (1) mountain area of high elevation which consists basically of Proterozoic rocks with high altitudes that might reach 2314 m (amsl) representing most of the basin's catchment area. This highly elevated area plays a significant role in the rainfall intensity

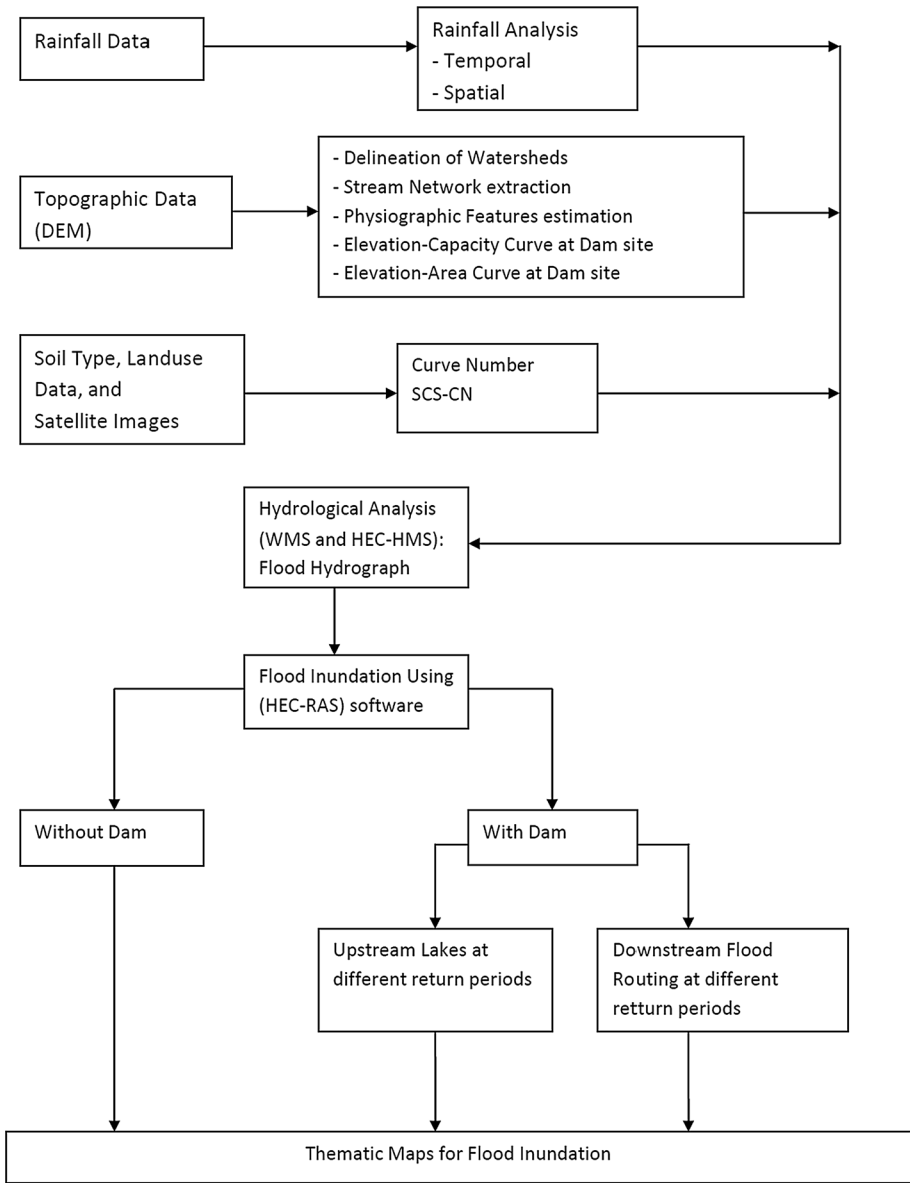


**Fig. 1** Flowchart of the proposed approach for rainfall–runoff, flood inundation modeling and flood risk assessment in arid zones

due to their orographic influence. (2) The hilly area that occupies the eastern and middle parts of the wadi is composed of hilly dissected and weathered rocks. (3) The Piedmont plains that occupy the low elevated parts between the high land and the Red Sea comprise morphotectonic depressions and main tributaries of the basin.

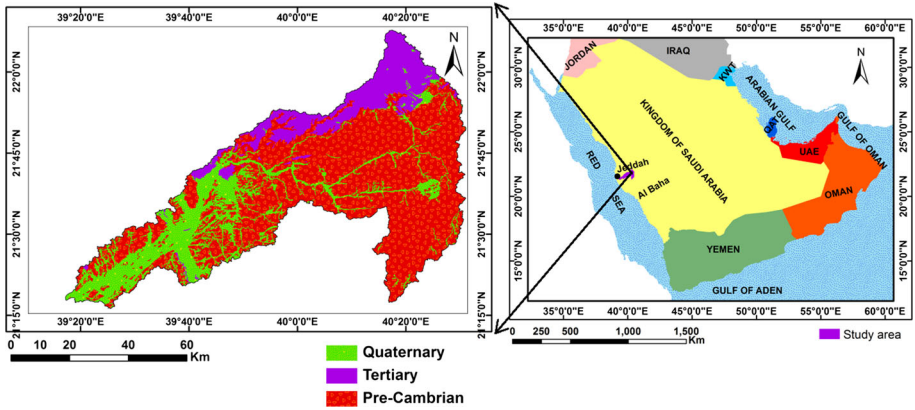


**Fig. 2** Location and geology of wadi Fatimah basin based on geological map of Makkah quadrangle sheet 21D (after Masoud et al. 2014)

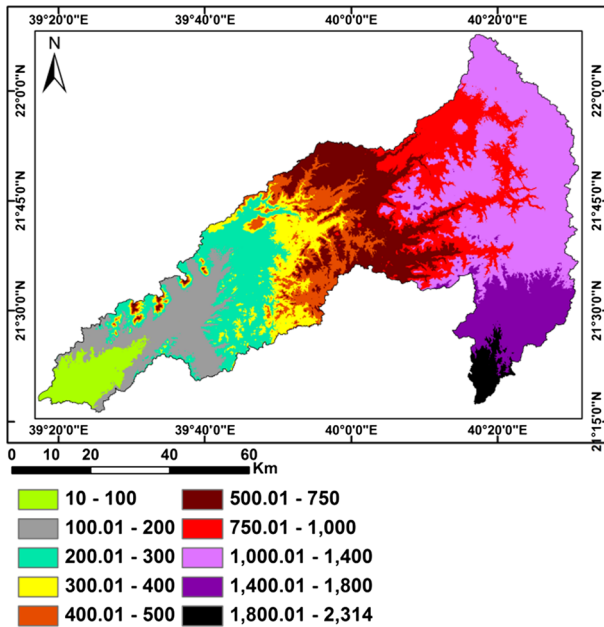


**Fig. 3** Digital elevation model (DEM) of wadi Fatimah basin (after Masoud et al. 2014)

### 4 Rainfall analysis

Rainfall data from eight stations that surround wadi Fatimah basin are used for development of temporal and spatial rainfall analyses. The available rainfall data include records for 40–45 years. To assess the flash flood of wadi Fatimah basin, the statistical analyses have been performed on the extremely daily rainfall amounts, using Weibull plotting position, followed by fitting various probability distributions to the data. Various frequency

distributions are fitted to the rainfall data to achieve the best distributions which fit the actual data of individual station. Distributions which have been evaluated in this study include normal, Gumbel, two-parameter log-normal, three-parameter log-normal, Pearson type III and log-Pearson type III distributions.

SMADA software (Eaglin 2012) is used to perform such an analysis. The best distributions are selected based on the root-mean-square error measure, RMSE (Chow et al. 1988), given by

$$\text{RMSE} = \sqrt{\frac{1}{n} \sum_{i=1}^n [\hat{R}_i - R_i]^2} \quad (1)$$

where  $R_i$  represents the actual precipitation amount of the measured station,  $\hat{R}_i$  represents the predictable precipitation amount based on the probability distributions, and  $n$  represents the number of data points of the gauged station.

RMSE values for the different distributions explain the mean inconsistency between the predictable value and the measured one. Table 1 shows the best fitting distributions depending upon the minimum RMSE as given by italicisation in the table. The best probability distribution is presented in Fig. 4. For the spatial analysis of rainfall, the inverse square distance weighting method (IDW) is applied for mapping the predictable rainfall depth at different recurrence periods of wadi Fatimah basin. A concise illustration of the methodology is specified by Viessman et al. (1977). Figure 5 shows maps of the spatial rainfall depth distributions over the study basin at different recurrence periods 5, 10, 25, 50 and 100 years, respectively. For more details about the methodology, a reference is made to Niyazi et al. (2014). The rainfall analysis presented by Wheater et al. (1989) has been also implemented for comparison reasons. In Wheater's approach, a spatial rainfall time series from point values of rainfall over the eight stations is obtained. Then, the formal statistical analysis has been implemented on the spatial rainfall depth. The statistical analysis shows that Pearson type III is the best distribution to fit the data based on the root-mean-square error. Table 2 summarizes the values of the design rainfall depth from both approaches. The results show an average difference of 5 mm between the design rainfall estimated in the current methodology (Niyazi et al. 2014) and the approach given by Wheater et al. (1989) for the different return periods 5, 10, 25, 50 and 100 years, respectively. This difference is not significant in arid regions.

**Table 1** Root-mean-square error (RMSE) of the rainfall stations at wadi Fatimah (after Niyazi et al. 2014)

Distribution type	Stations							
	J 102	J 113	J 114	J 204	J 205	J 208	J 214	J 239
Normal	1.18	2.53	1.78	1.03	0.98	0.81	1.47	0.7
Two-parameter log-normal	0.7	<i>1.43</i>	1.69	0.66	0.97	0.55	0.82	0.75
Three-parameter log-normal	0.67	1.47	1.4	0.6	0.67	0.56	0.81	0.5
Pearson type III	<i>0.65</i>	1.48	1.36	<i>0.55</i>	<i>0.62</i>	0.55	<i>0.73</i>	<i>0.45</i>
Log-Pearson type III	1.01	1.48	1.44	0.89	1.6	0.69	1.18	0.57
Gumbel type I	0.75	1.72	<i>1.14</i>	0.61	0.71	<i>0.52</i>	0.91	0.49

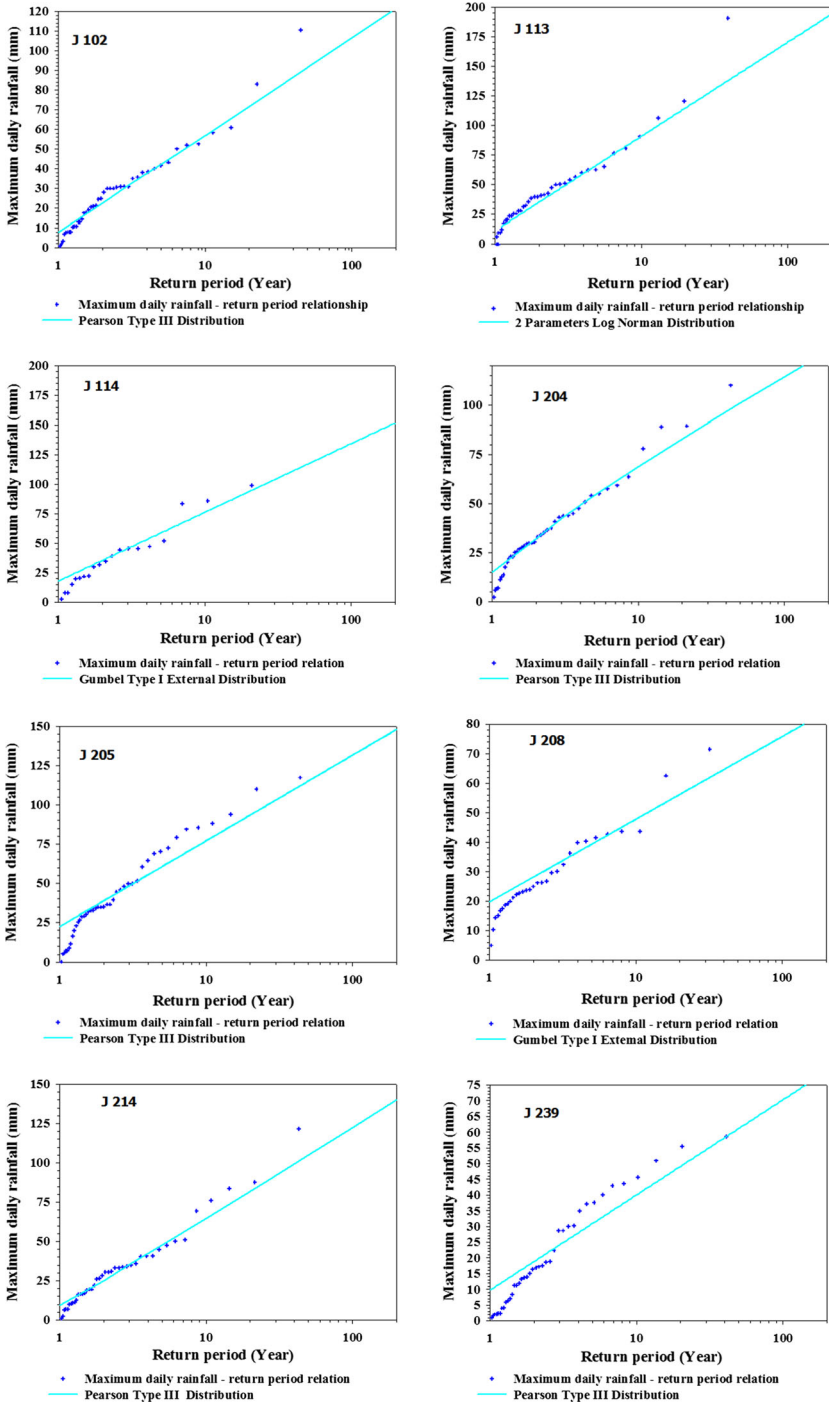


**Fig. 4** Rainfall depth frequency analysis at the stations in the study area based on the best probability distribution assigned from Table 1 (modified from Niyazi et al. 2014)

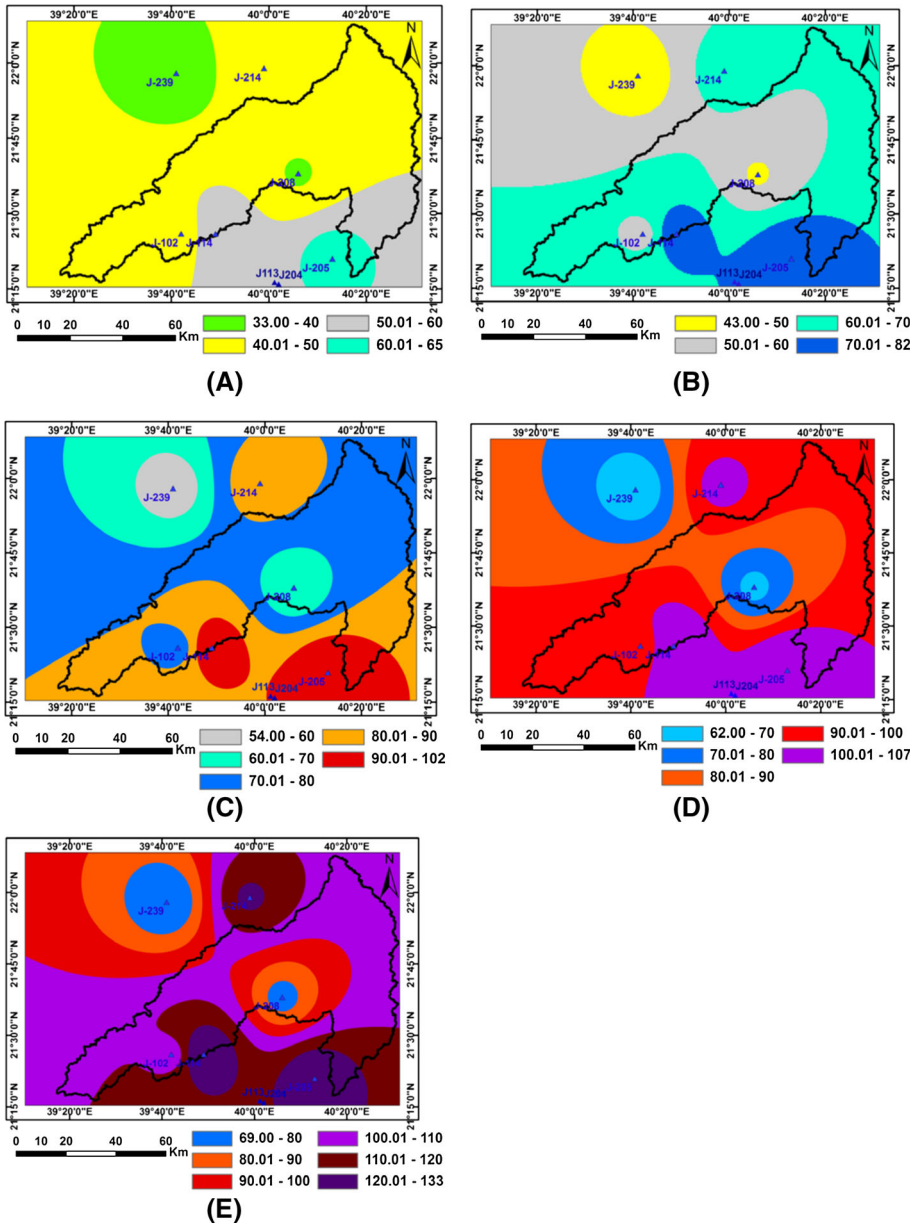


**Fig. 5** Mapping of the expected rainfall depth at different return periods: **a** 5 years, **b** 10 years, **c** 25 years, **d** 50 years and **e** 100 years (modified from Niyazi et al. 2014)

### 5 Assessment of land use, land cover and curve number (CN)

Surface runoff is defined as the rainfall excess after subtracting the initial and additional abstractions results from evaporation and infiltration, respectively. Both the infiltration and the potential maximum retention are based on the physical properties of the soil and land



**Table 2** Rainfall depth over the wadi for different return periods

Return period (years)	5	10	25	50	100
Spatial average rainfall depth (mm) based on the current study	44	52.6	62.6	68.6	76.7
Spatial rainfall depth (mm) based on Wheater et al. (1989)	37.5	46.2	56.6	64	71.1

surface features of the basin. Physical properties of the soil include textures, compactions, structures and soil moistures, while surface features include land use, land cover and the topographic characteristics. Consequently, flash flood amounts depend upon rainfall, soil characteristics, land use, land cover and relief. The Soil Conservation Services (SCS) of the USA (lately renamed as Natural Resources Conservation Services, NRCS) issued a mathematical formula for calculating runoff of hydrographic basin and named SCS Runoff CN scheme as follows:

$$Q = (P - 0.2S)^2 / (P + 0.8S) \tag{2}$$

where  $Q$  represents the surface runoff amount,  $P$  represents the rainfall amount, while  $S$  represents the potential maximum retention amount.

The potential maximum retention is estimated through the hydrological element named curve number (CN) as follows:

$$S = (25400/CN) - 254 \tag{3}$$

where CN is the curve number.

The curve number (CN) is a mathematical value of hydrological element which describes the potentiality of flash flood of the hydrographic basin. The CN is influenced by physical properties of the soil, land use, land cover and soil moisture aspects. So, the CN is considered as a hydrological parameter that expresses about the combination of hydrological soil groups and land use.

As reported by Masoud (2016), based upon the NRCS, soils are grouped into four groups and each group called by a letter as A, B, C and D with particular features for each group. The A soil group includes deep sands, deep loess, and silt. The B soil group includes shallow loess and sandy loam. The C soil group comprises of clay loam, shallow sandy loam, soils of low organic content with high amount of clay. The D soil group includes soils that are swelling up considerably when getting wet which is comprises clay and salty soils. The NRCS soil group is able to be identified at the site using either soil properties or the country soil maps. In this study, soil groups could classify depending upon the soil maps of the Ministry of Agriculture and land use analyses of the areal images.

The resulted soil maps and land use diversity of the study area (Fig. 6a, b, respectively) show that about 80 % of the basin’s area is bare soil. The northern parts at the upstream of the basin contain bush and grass cover and occupy about 15 % of the total area. Some scattered of residential areas is about 10 % of the total area particularly in the lower third of the basin toward the western direction. Farm lands are very restricted in wadi Fatimah and occupy some scattered small portion around the main tributaries with an area of about 5 % of the total area. The calculated value of the weighted mean CN for wadi Fatimah basin which is used for the hydrological analysis is shown in Table 3.

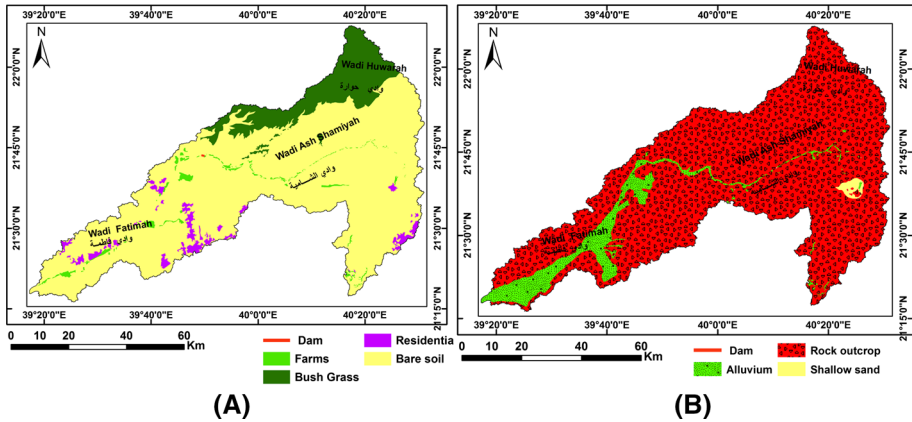


**Fig. 6** Wadi Fatimah land use and soil types maps: land use (a) and soil types (b)

### 6 Wadi Fatimah Dam

Wadi Fatimah Dam consists of four main components: (1) the dam body which is made up of concrete. It is a gravity-type dam. (2) Dam spillway that protects the dam and releases the flood safely over the spillway crest, (3) the dam outlet near the dam bottom, that helps in emptying the dam reservoir when the reservoir is full of water, and (4) the dam stilling basin that is downstream of the dam to dissipate the water energy either released from the spillway or the dam outlets to protect the downstream channel from erosion and consequently protect the dam from overturning failure. The dam properties are presented in Table 4, and Fig. 7 shows images of the aforementioned four components during the visit by the project team.

### 7 Rainfall–runoff modeling

Two hydrological models are applied to wadi Fatimah basin to assess the flash flood volumes which result from the rainfall events of recurrence time intervals 5, 10, 25, 50 and 100 years. Due to the scarcity of the hydrological measurements, model of this study is

**Table 3** Estimation of the weighted average CN over the catchment until the dam

No.	Matrix calculating CN Land use—soil type	CN <sub>i</sub>	Area (km <sup>2</sup> ) (A <sub>i</sub> )	Area (%)	Weighted CN <sub>i</sub> for each area
1	Bare soil—alluvium	63	46.25	1.5	1.0
2	Bare soil—shallow sand	85	30.814	1.0	0.9
3	Bare soil—rock outcrops	88	2370.37	78.0	68.7
4	Bush grass—rock outcrops	55	530.18	17.5	9.6
5	Farms—alluvium	74	23.97	0.8	0.6
6	Farm—rock outcrop	86	6	0.2	0.2
7	Residential—rock outcrops	87	29.92	1.0	0.9
Total			3037.01	100	82

**Table 4** Wadi Fatimah Dam properties (from the dam plate at the site)

Dam property	Value
Dam height (m)	15 m
Dam length (m)	600 m
Dam capacity	20 million cubic meters
Dam spillway type	Ogee spillway



**Fig. 7** Images of wadi Fatimah Dam: *Top left* (general dam view), *top right* (part of the dam spillway), *bottom left* (dam outlet looking from upstream) and *bottom right* (dam stilling basin with baffle blocks and end-danted sills)

depending upon the conjunction between geographic information system (GIS), watershed modeling system (WMS 7.1) and hydrological modeling system (HEC-HMS 3.3). WMS 7.1 has been issued by the Environmental Modeling Research Laboratory of Brigham Young University, can delineate the basin catchment and water divides, and calculate the morphometric parameters. GIS helps for other computations, contouring, cross sections extraction from digital elevation model, creation of thematic maps and rainfall distribution analysis. More information about the model is available at Environmental Modeling Research Laboratory (1998). HEC-HMS 3.5 has been issued by the US Army Corps of Engineers and is able to evaluate the relationship between the rainfall and runoff of the hydrographic basins. HEC-HMS has different options that allow the user to select between numerous losses and unit hydrograph parameterizations (HEC 2000). One of these hydrograph parameterizations is the SCS-CN scheme which is used for estimation of the runoff volume. SCS hyetographs type II is usually applied for the arid and semi-arid catchments to study the distribution of rainfall events at specific duration. Figure 8 displays

the hyetograph of rainfall events and the equivalent flash flood hydrograph with different recurrence time intervals. The modeled peaks of discharge at the dam site are 446.5, 702.2, 1068.2, 1288.2 and 1593.4 m<sup>3</sup>/s for 5, 10, 25, 50 and 100 years, respectively. The equivalent flash flood volumes are 23.7, 37.2, 56.6, 68.2 and 84.3 million cubic meters, respectively. Since the dam capacity is 20 million cubic meters (Table 4), this volume corresponds to about 5-year return period.

### 8 Flood inundation modeling (FIM)

FIM of wadi Fatimah basin is based upon two concepts of both upstream and downstream sides of the dam. For the upstream side of the dam, two capacity curves of inundated area and its elevation and the volume of runoff with the elevation have been constructed from

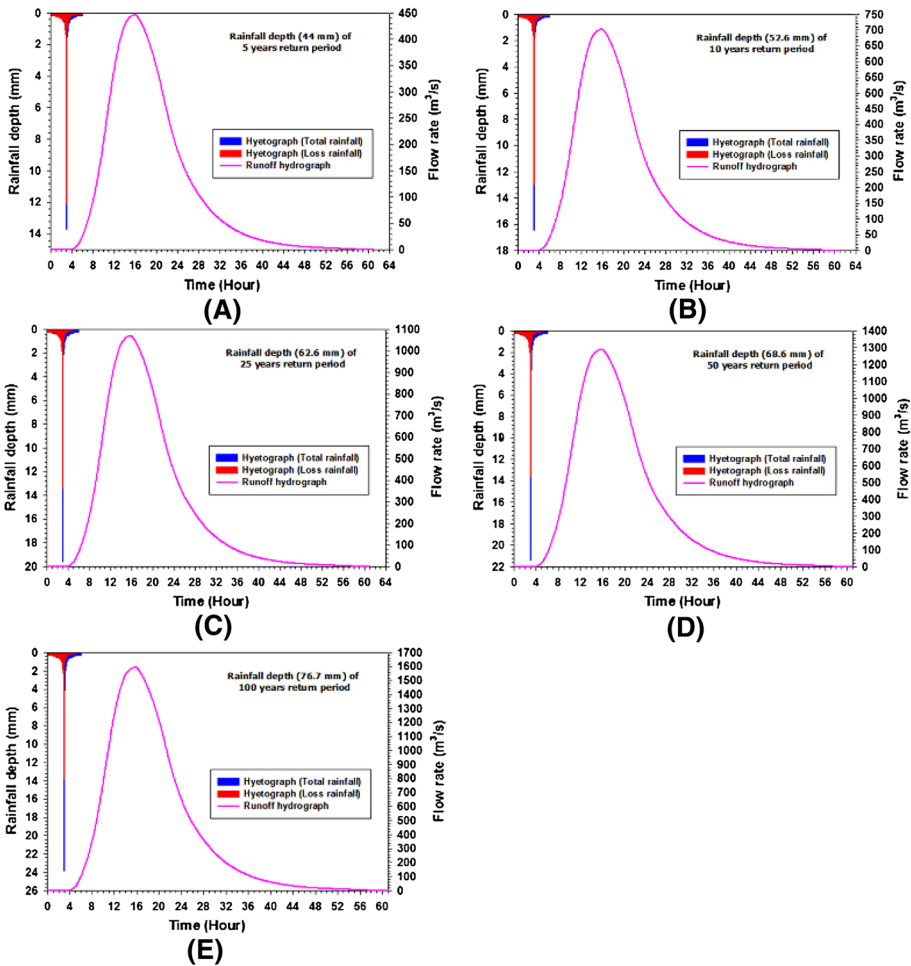


**Fig. 8** Rainfall hyetographs and the corresponding flood hydrographs at different return periods: **a** 5 years, **b** 10 years, **c** 25 years, **d** 50 years and **e** 100 years)

the digital elevation model at the dam site using WMS software. Figure 9 shows both the capacity curves at the dam lake which are the characteristics of the dam reservoir. The curve of the relation between the area and the elevation shows some irregular leaps which mean that there is no change in these areas with changing elevations. This irregularity of this curve is due to the mountains and hilly areas which have steep slope at those leaps.

Figure 8 shows the modeled hydrographs by HEC-HMS with the estimated flash flood volumes at different return periods with the equivalent water surface elevation estimated from the curve in the right-hand side of Fig. 9. Elevations of the reservoir lake have been estimated and are about 294, 297, 302, 304 and 306 m at return periods of 5, 10, 25, 50 and 100 years. Using GIS techniques, the inundation areas for the dam lake are delineated and displayed in Fig. 10 for the designated return periods.

Flood analysis at the downstream side of the dam has been performed using HEC-RAS software which has been issued by US corps of engineers. The software considers as a hydraulic modeling package that has the ability to carry out steady and non-steady flow modeling with one-dimensional river and flood inundations. For this research, a steady flow is applied to delineate the inundations area at the dam downstream. According to Brunner (2010), the progressive variation of flow formula is applied in HEC-RAS to compute the profile of surface runoff through group of cross sections along the main valley of the basin from one to the other based upon the energy equations with a reiterated ideal step method, and this energy formula of steady-state flow is as follows:

$$Z_2 + Y_2 + \frac{\alpha_2 V_2^2}{2g} = Z_1 + Y_1 + \frac{\alpha_1 V_1^2}{2g} + h_e \tag{4}$$

where  $Z_1$  and  $Z_2$  represent the channel elevation values,  $Y_1$  and  $Y_2$  represent the water depths at cross sections,  $V_1$  and  $V_2$  represent the mean velocity values at the cross sections of the channel,  $\alpha_1$  and  $\alpha_2$  represent the velocity weighting coefficient values at the channel cross section,  $g$  is the acceleration as a result of gravity, and  $h_e$  represents the energy head loss which is calculated by Manning formula as reported by Masoud (2016),

$$h_e = L \left( \frac{Qn}{AR^{2/3}} \right)^2 \tag{5}$$

where  $Q$  represents the runoff discharge along the channel,  $A$  represents the cross-sectional area of the channel,  $R$  represents the hydraulic radius of the channel cross section,

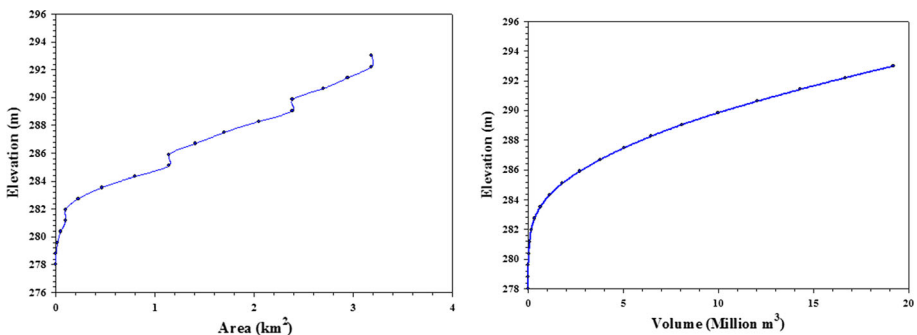
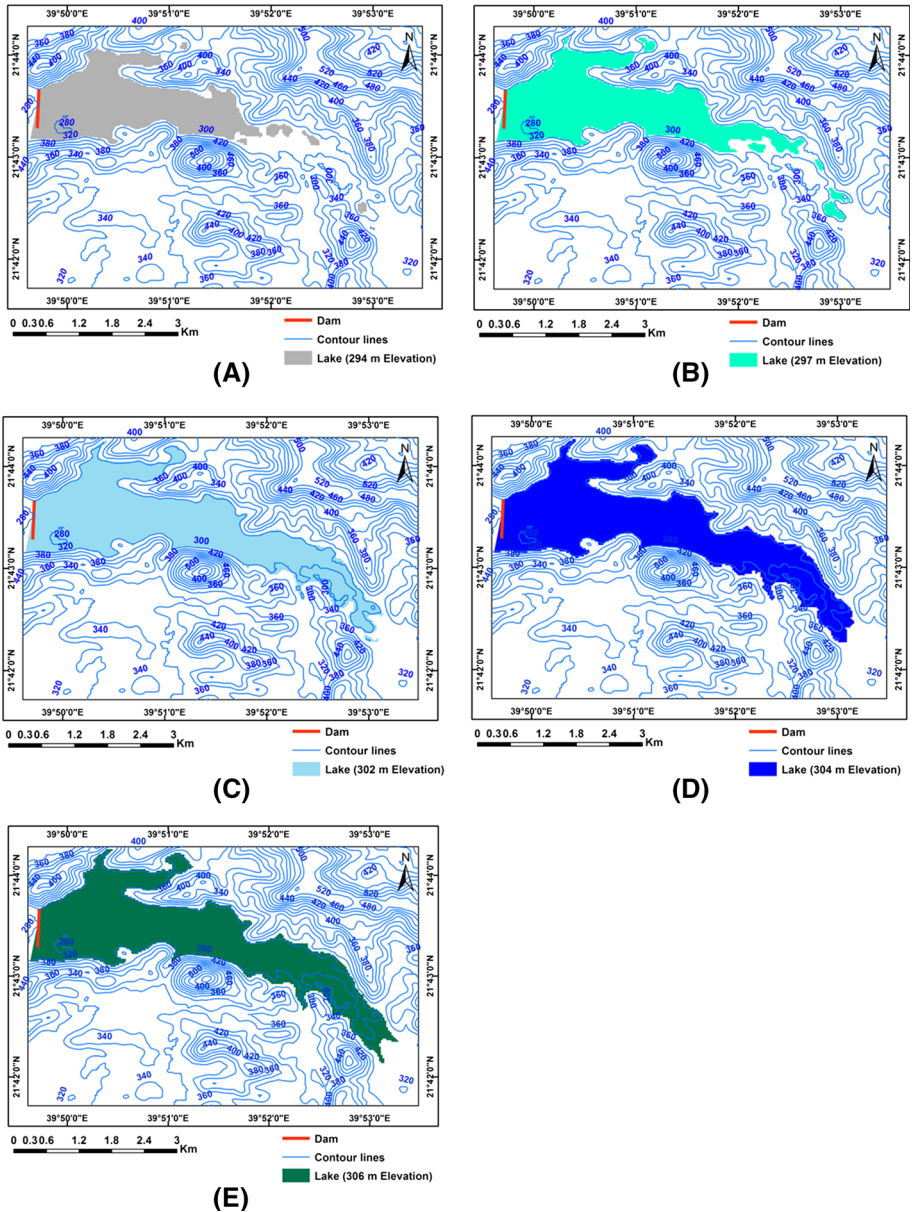


Fig. 9 The surface area–elevation and the capacity–elevation curves of the dam reservoir



**Fig. 10** Dam lake shape in the upstream side of the dam and inundation areas at different return periods: **a** 5 years (lake area = 3.7 km<sup>2</sup>), **b** 10 years (lake area = 4.4 km<sup>2</sup>), **c** 25 years (lake area = 5.6 km<sup>2</sup>), **d** 50 years (lake area = 6.2 km<sup>2</sup>) and **e** 100 years (lake area = 6.4 km<sup>2</sup>)

*n* represents Manning roughness coefficient, and *L* represents the distance between the two consecutive cross sections.

Figure 11 explains the elements of the energy formula, and the above-mentioned formulas have been applied and solved between two consecutive cross sections along the main channel for estimating the water depth and velocities.



It should be noted here that the current study focuses on a parsimonious approach for flood mapping since the data are limited in such an arid area. However, the uncertainty in the model parameters such as the study given by Pappenberger et al. (2006) is beyond the scope of the current work.

Figure 12 shows the channel path from the dam toward the downstream and the bottom topography of the channel used in the model of inundations. The downstream channel length is 80 km and has been separated into 39 cross sections for the progressive flow variations (Fig. 13). The mean interval between two following cross sections is equal to 2 km and may vary between the cross sections depending on the variations of the flow direction, taking into consideration the cross section must be perpendicular to direction of flow along the channel. To study the influence of the dam construction upon the flooding area and to evaluate the flash flood hazardous, two scenarios have been created. The initial scenario supposes dam absence (it is called “without dam” in Table 5), while the second scenario is the presence of the dam representing the current situation (it is called “with dam” in Table 5). In both cases, the five storm return periods were considered. The data and the results of the two scenarios with the five storm return periods are presented in Table 5.

### 9 Dam reservoir routing

Since the hydrographs calculated by HEC-HMS and presented in Fig. 8 are the hydrographs at the upstream side of the dam, a reservoir routing technique is required to route the hydrograph over the spillway to the downstream channel. The storage indication method called “Modified Plus Method” is used to perform the flood routing (Viessman et al. 1977; Chow et al. 2002). A brief description of this method is given below. Flow over an ungated spillway can be described from energy and continuity equation of the fluid flow by the form (Chow 1959),

$$O = \frac{2}{3} C_d B \sqrt{2g} H^{1.5} \tag{6}$$

where  $O$  is the outflow rate,  $C_d$  is the discharge coefficient,  $B$  is the spillway crest length,  $H$  is the hydraulic head over the crest, and  $g$  is the acceleration due to gravity.

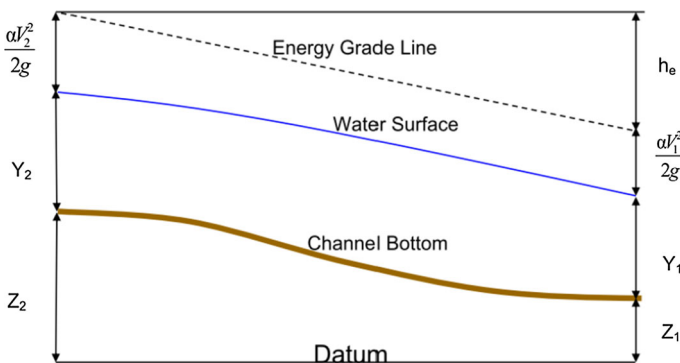
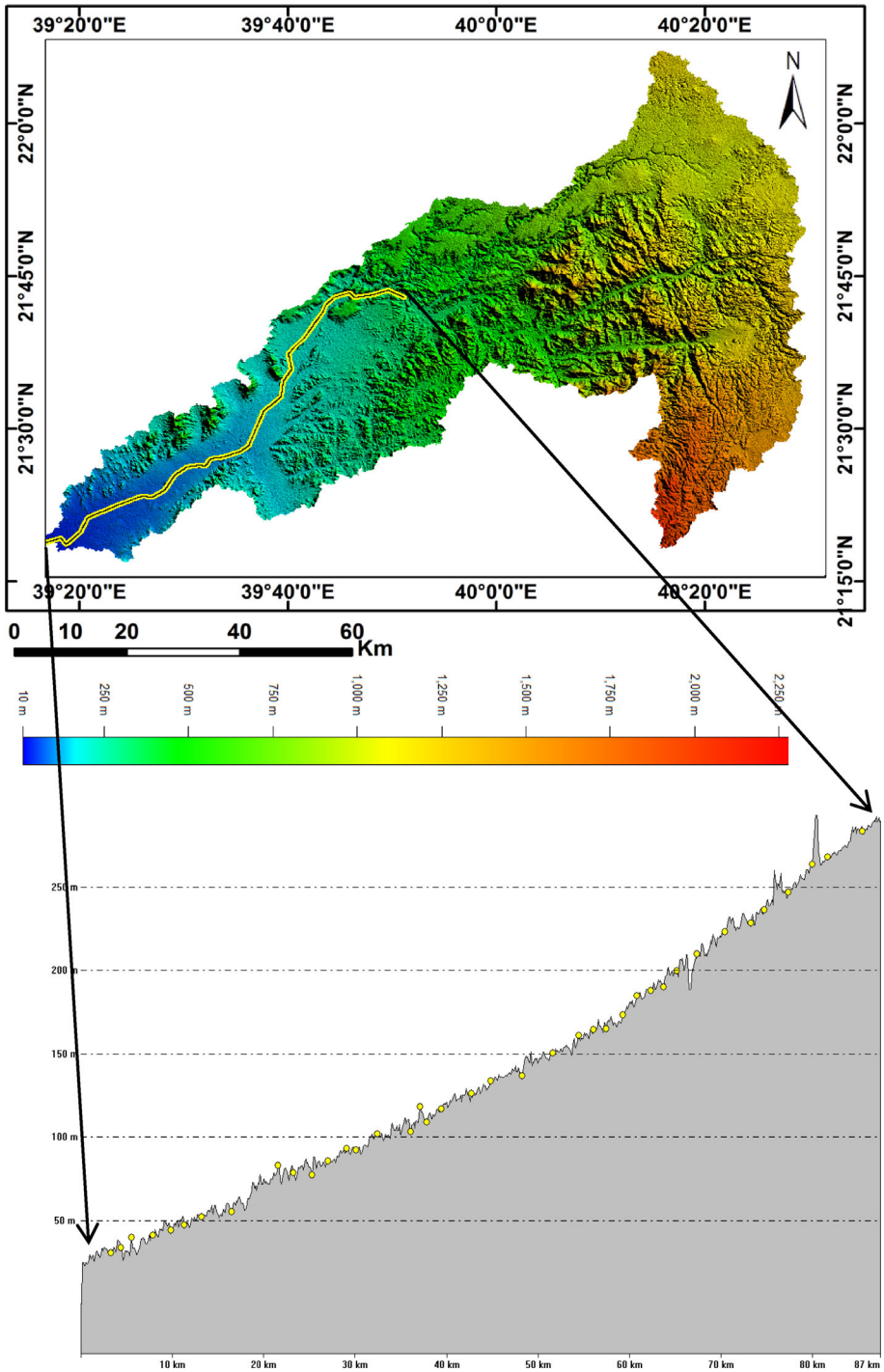
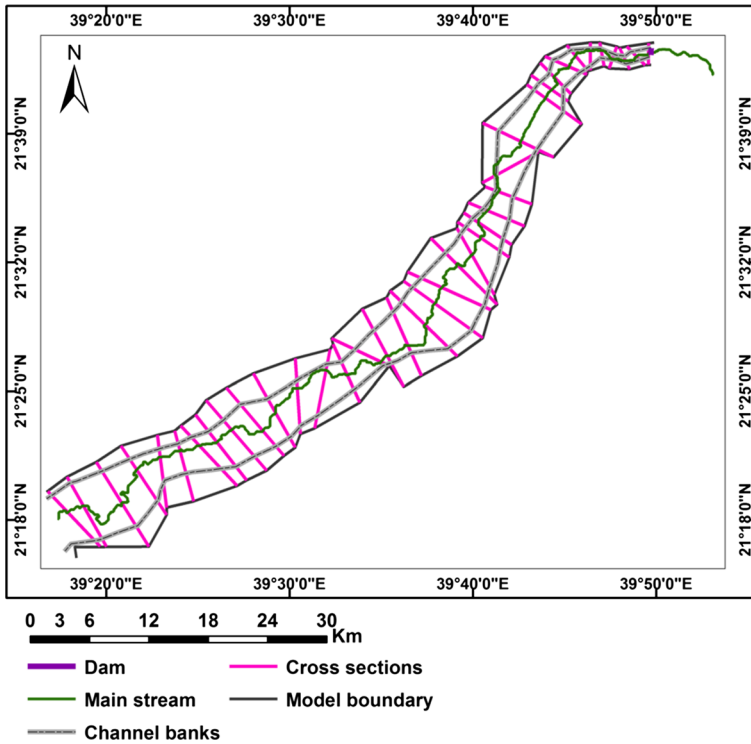


Fig. 11 Representation of the terms in the energy equation (after Brunner 2010)



**Fig. 12** The downstream channel after the dam and the longitudinal profile of the channel *bottom* from the DEM. The *color scale* represents the elevations in the catchment





**Fig. 13** The cross sections in the downstream channel after the dam and the model boundary conditions. *Note* the cross sections are locally perpendicular to the flow path

Since storage and outflow both depend only on the reservoir elevation, the resulting storage–elevation curve (Fig. 9) and outflow–elevation relationship (Eq. 6) can be combined to produce a storage–outflow graph. The reservoir routing method relies on the mass conservation given by the well-known storage equation,

$$I - O = \frac{dS}{dt} \tag{7}$$

where  $I$  is the inflow rate to the reservoir,  $O$  is the outflow rate from the reservoir,  $S$  is the surcharge storage in the reservoir, and  $dS/dt$  is the rate of change of the storage within the reservoir.

For computational purposes, Eq. (7) is written in a finite difference form as,

$$\frac{I_{t+\Delta t} + I_t}{2} - \frac{O_{t+\Delta t} + O_t}{2} = \frac{S_{t+\Delta t} - S_t}{\Delta t} \tag{8}$$

where  $\Delta t$  is the incremental time step used in the computations.

Equation (8) can be rearranged in a way to provide the unknown terms in one side of the equation and the known terms on the other side to read,

$$I_{t+\Delta t} + I_t + \left( \frac{2S_t}{\Delta t} - O_t \right) = \frac{2S_{t+\Delta t}}{\Delta t} + O_{t+\Delta t} \tag{9}$$

In this equation, only unknown term for any time interval is the term on the right-hand side. A trial-and-error method could be applied to solve the above equation (Viessman et al.

**Table 5** Summary of the scenarios considered in the study and their overall results

Return period (years)	Total rainfall (mm)	Without dam				With dam			
		Maximum Q (m <sup>3</sup> /s)	Volume (10 <sup>6</sup> m <sup>3</sup> )	Average depth (m)	Inundation area (km <sup>2</sup> )	Maximum Q (m <sup>3</sup> /s)	Volume (10 <sup>6</sup> m <sup>3</sup> )	Average depth (m)	Inundation area (km <sup>2</sup> )
5	44	446.50	23.70	1.6	92.00	348.60	23.70	1.4	67.20
10	52.6	702.20	37.20	1.9	99.30	548.70	37.20	1.7	76.70
25	62.6	1068.20	56.60	2.2	124.80	834.00	56.60	2	93.20
50	68.6	1288.20	68.20	2.4	153.40	1005.90	68.20	2.2	102.70
100	76.7	1593.40	84.30	2.7	161.00	1244.30	84.30	2.4	137.30

1977); therefore, pairs of trial values for  $S_{t+\Delta t}$  and  $O_{t+\Delta t}$  could be generated that satisfy Eq. (7) or storage indication curve (storage–outflow) could be drawn to have a direct determination of  $O_{t+\Delta t}$  once a value of  $2S_{t+\Delta t}/\Delta t + O_{t+\Delta t}$  has been calculated. A spreadsheet has been developed to perform the computation given by Eq. (7). The results of this process are given in Fig. 14. The figure shows the results of the dam reservoir routing at different return periods. The figure shows the attenuation of the flood peak and the delay of the flood peak due to the reservoir storage effect. In the current study, the authors considered the case that the dam reservoir is full (the worst case). This is the common scenario (Viessman et al. 1977). A summary of the routing effect in terms of flood peak and flood volume is presented in Table 5. It should be noted that the inflow volume should be equal to the outflow volume, while the peak discharge is attenuated. The values of the peak flows are used later on in the flood inundation modeling using HEC-RAS in the two scenarios.

Figure 15 shows the inundated area computed by HEC-RAS for the two scenarios at the five return periods. It is obvious from the figure that the inundated area is reduced due to the existence of the dam. For flood mitigation, these areas should be protected from floods either by the construction of flood wall defense or by expropriating these areas and

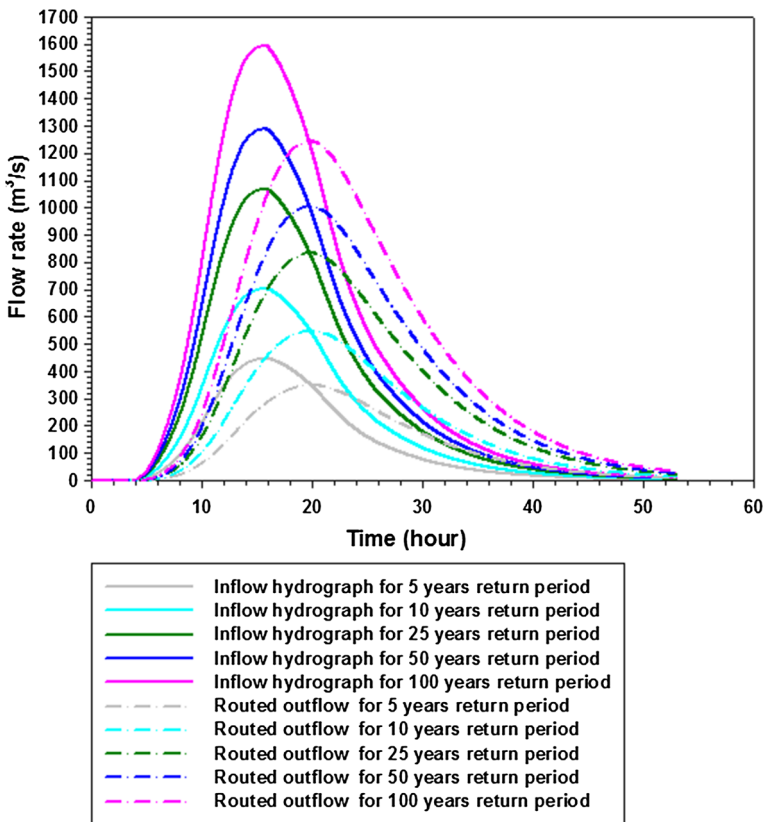


**Fig. 14** Dam reservoir routing over the dam spillway for inflow hydrograph at different return periods

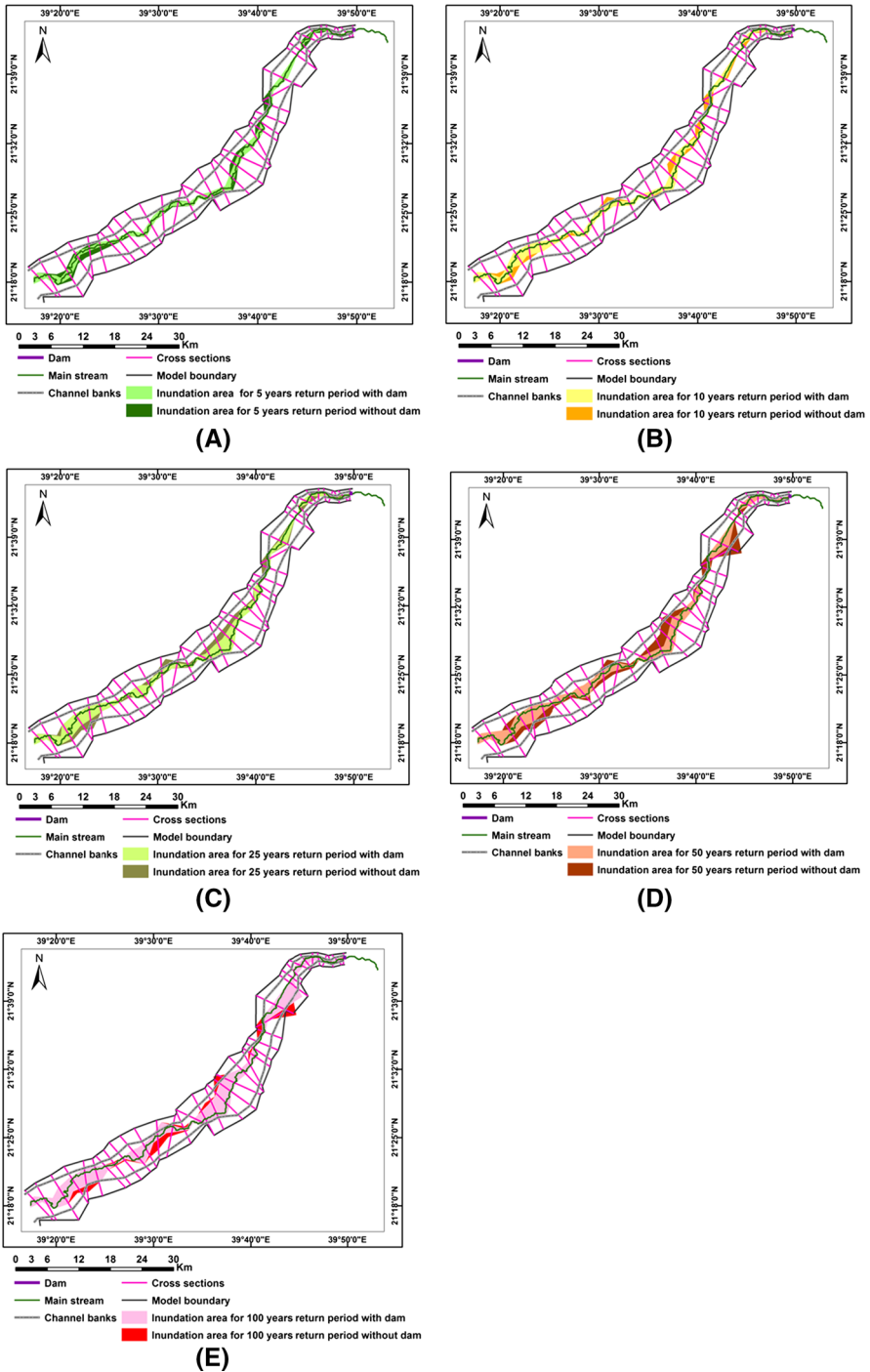


**Fig. 15** Flood inundation areas downstream of the dam at different return periods with and without the dam: **a** 5 years, **b** 10 years, **c** 25 years, **d** 50 years and **e** 100 years

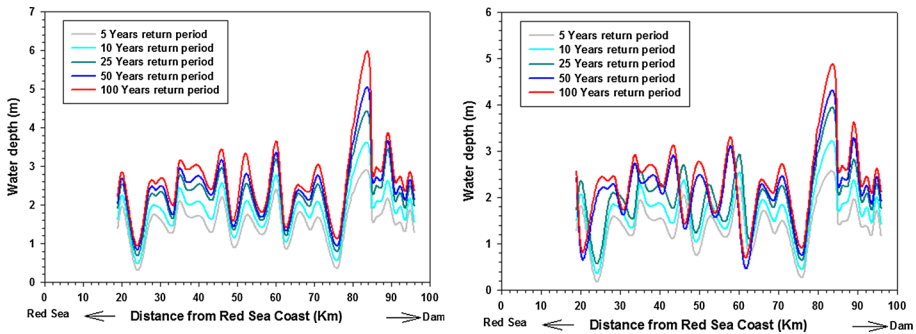


**Fig. 16** Water depth distribution over the downstream channel, *left image* without dam and *right image* with dam

preventing building residential areas in these places. Table 5 shows the inundated area with and without the dam. The reduction in the inundation area varies in each return period, but generally resides within 25 %. Figure 16 shows the water depth along the channel reach for different return periods with and without the presence of the dam. It is obvious that the water depth increases from 5-year return period to 100-year return period. The results of the average water depth at different return periods are also presented in Table 5. It is found that the presence of the dam reduces the water depth by about 10 % on average along the channel for the considered return periods.

### 10 Summary and conclusions

This paper presents an integrated approach that couples two types of hydrological models which are dealing with relationship between rainfall and surface runoff simulation mutually with FIM to assess the flash flood hazard in arid regions with the absence of measured hydrological information. Wadi Fatimah basin is situated in the western part of Saudi Arabia and was selected as a case study to examine the integration of hydrological models and GIS techniques. Some concluded remarks could be find out through this research as follows: (1) The mathematical analyses of rainfall distributions and surface runoff information prove that there are some stations that do not follow Gumbel distribution, which is considered well known for the rainfall measurements in Saudi Arabia. (2) Evaluated results show that the dam of wadi Fatimah basin has been constructed for storage capacity  $\leq 5$ -year recurrence time interval. (3) It is p that the occurrence of the dam can reduce the mean water depth by about 10 % along the main valley of wadi Fatimah basin at 5-year recurrence interval time. Results show that the mean reduction of the inundation areas due to the constructed dam is about 25 %. It could be concluded that the scheme of integration of the hydrological model, GIS techniques and FIM is a practical and helpful tool to evaluate the dam construction and flash flood hazard of arid and semi-arid regions with limitation or the absence of measured hydrological information.

**Acknowledgments** This project was funded by the Deanship of Scientific Research (DSR), King Abdulaziz University, Jeddah, under Grant No. 416/155/1434. The authors, therefore, acknowledge with thanks DSR technical and financial support.

## References

- Al Saud M (2009) Morphometric analysis of Wadi Aurnah drainage system western Arabian Peninsula. *Open Hydrol J* 3:1–10
- Al Yamani MS (2004) Hydraulic response of wadi Fatimah basin, western province, Kingdom of Saudi Arabia. *Arab Gulf J Sci Res* 22(3):157–164
- Al-Ahmadi FS (2005) Rainfall-runoff modeling in arid regions using GIS and RS. Case study: western of Saudi Arabia. M.Sc. thesis, King Abdulaziz University, Saudi Arabia
- Brunner GW (2010) HEC-RAS, river analysis system hydraulic reference manual. USACE-HEC, Davis
- Chow VT (1959) Open channel hydraulics. McGraw-Hill, New York
- Chow VT, Maidment DR, Mays L (1988) Applied hydrology. McGraw-Hill, New York
- Chow VT, Maidment DR, Mays LW (2002) Applied hydrology. McGraw-Hill, New York
- Collier C (2007) Flash flood forecasting: what are the limits of predictability? *Q J R Meteorol Soc* 133(622A):3–23
- Creutin JD, Borga M (2003) Radar hydrology modifies the monitoring of flash flood hazard. *Hydrol Process* 17(7):1453–1456. doi:10.1002/hyp.5122
- Eaglin R (2012) SMADA software. UCF rainfall analysis. <https://ucf-rainfall.pbworks.com/w/page/9654987/FrontPage>
- El Osta MM, Masoud HM (2015) Implementation of a hydrologic model and GIS for estimating Wadi runoff in Dernah area, Al Jabal Al Akhadar, NE Libya. *J Afr Earth Sci* 107:36–56. doi:10.1016/j.jafrearsci.2015.03.022
- Environmental Modeling Research Laboratory (EMRL) (1998) Watershed modeling system (WMS), reference manual and tutorial
- Fernandez D, Lutz M (2010) Urban flood hazard zoning in Tucumán Province, Argentina, using GIS and multicriteria decision analysis. *Eng Geol* 111(1–4):90–99
- Georgakakos KP (1992) Advances in forecasting flash floods. In: Proceedings of the CCNAA-AIT joint seminar on prediction and damage mitigation of meteorologically induced natural disasters, 21–24 May 1992, National Taiwan University, Taipei, Taiwan, pp 280–293
- Guzzetti F, Tonelli G (2004) Information system on hydrological and geomorphological catastrophes in Italy (SICI): a tool for managing landslide and flood hazards. *Nat Hazards Earth Syst Sci* 4:213–232
- He YP, Xie H, Cui P, Wei FQ, Zhong DL, Gardner JS (2003) GIS-based hazard mapping and zonation of debris flows in Xiaojiang Basin, southwestern China. *Environ Geol* 45(2):286–293
- HEC (2000) Hydrologic modeling system: technical reference manual. US Army Corps of Engineers Hydrologic Engineering Center, Davis
- Horton RE (1932) Drainage basin characteristics. *Trans Am Geophys Union* 13:350–361
- Horton RE (1945) Erosional development of streams and their drainage basins: hydrophysical approach to quantitative morphology. *Geol Soc Am Bull* 56:275–370
- Masoud MH (2015) Rainfall-runoff modeling of ungauged Wadis in arid environments (case study Wadi Rabigh-Saudi Arabia). *Arab J Geosci* 8(5):2587–2606. doi:10.1007/s12517-014-1404-0
- Masoud MH (2016) Geoinformatics application for assessing the morphometric characteristics' effect on hydrological response at watershed (case study of Wadi Qanunah, Saudi Arabia). *Arab J Geosci* 9:280. doi:10.1007/s12517-015-2300-y
- Masoud M, Niyazi B, Elfeki A, Zaidi S (2014) Mapping of flash flood hazard prone areas based on integration between physiographic features and GIS techniques (case study of Wadi Fatimah, Saudi Arabia). In: 6th International conference on water resources and the arid environments (ICWRAE 6), pp 334–347, 16–17 Dec 2014, Riyadh, Saudi Arabia
- Merzi N, Aktas MT (2000) Geographic information systems (GIS) for the determination of inundation maps of Lake Mogan, Turkey. *Water Int* 25(3):474–480
- Nageswararao K, Swarna LP, Arun KP, Hari KM (2010) Morphometric analysis of Gostani River basin in Andhra Pradesh State, India using spatial information technology. *Int J Geomat Geosci* 1(2):79–187
- Niyazi B, Elfeki A, Masoud M, Zaidi S (2014) Spatio-temporal rainfall analysis at Wadi Fatimah for flood risk assessment. In: 6th international conference on water resources and the arid environments (ICWRAE 6), pp 308–314, 16–17 Dec 2014, Riyadh, Saudi Arabia
- Pappenberger F, Matgen P, Beven KJ, Henry JB, Pfister L, Fraipont P (2006) Influence of uncertain boundary conditions and model structure on flood inundation predictions. *Adv Water Resour* 29(10):1430–1449
- Rudriaih M, Govindaiah S, Srinivas Vittala S (2008) Morphometry using Remote sensing Techniques in the sub-Basins of Kagna River Basin, Gulburga District, Karnataka, India. *J Indian Soc Remote Sens* 36(12):351–360

- Sanyal J, Lu X (2006) GIS-based flood hazard mapping at different administrative scales: a case study in Gangetic West Bengal, India. *Singap J Trop Geogr* 27:207–220
- Şen Z, Khiyami AH, Al-Harthy SG, Al-Ammawi FA, Al-Balkhi AB, Al-Zahrani MI, Al-Hawsawy HM (2012) Flash flood inundation map preparation for Wadi in arid regions. *Arab J Geosci*. doi:[10.1007/s12517-012-0614-6](https://doi.org/10.1007/s12517-012-0614-6)
- Strahler AN (1964) Quantitative geomorphology of drainage basins and channel networks. *Handbook of applied hydrology*. McGraw Hill, New York
- Subyani AM (2009) Hydrologic behavior and flood probability for selected arid basins in Makkah area, western Saudi Arabia. *Arab J Geosci*. doi:[10.1007/s12517-009-0098](https://doi.org/10.1007/s12517-009-0098)
- Sui DZ, Maggio RC (1999) Integrating GIS with hydrological modeling: practices, problems, and prospects. *Comput Environ Urban Syst* 23:33–51
- Viessman W, Knapp JW, Lewis GL, Harbaugh TE (1977) *Introduction to hydrology*. Happer and Row Publishers, New York
- Wheater HS, Laurentis P, Hamilton GS (1989) Design rainfall characteristics for South-West Saudi Arabia. *Proc Inst Civ Eng* 87(4):517–538
- Younis J, Anquetin S, Thielen J (2008) The benefit of high resolution operational weather forecasts for flash-flood warning. *Hydrol Earth Syst Sci Discuss* 5:345–377
- Zerger A, Smith DI (2003) Impediments to using GIS for real-time disaster decision support. *Comput Environ Urban Syst* 27:123–141